Available online at www.sciencedirect.com

Journal of Photochemistry and Photobiology A: Chemistry 178 (2006) 150–155

Journal of Photochemistry and Photobiology A:Chemistry

www.elsevier.com/locate/jphotochem

The relaxation dynamics of the excited state of stilbene dendrimers substituted with phenylacetylene groups

Yoshinobu Nishimura [a], Masafumi Kamada [a], Masashi Ikegami [a], Ritsuko Nagahata [b], Tatsuo Arai [a,*]

[a] *Graduate School of Pure and Applied Sciences, University of Tsukuba, Tsukuba, Ibaraki 305-8571, Japan*
[b] *Research Center of Macromolecular Technology, National Institute of Advanced Industrial Science and Technology (AIST), Tsukuba 305-8565, Japan*

Abstract

Energy migration and emitting processes of a series of dendrimers linked by a phenylacetylene group bearing stilbene as a core were investigated by steady state and time-resolved fluorescence spectroscopy. In higher generation, we confirmed efficient energy migration from peripheral moiety to a core followed by emission with high quantum yield. The kinetics of emitting state was also examined by lifetime measurement and revealed generation dependence of fluorescence decay constants. In the case of higher generation, peripheral moieties might be involved in relaxation process in the excited state in contrast to negligible interaction to the core in the ground state.

Keywords: Dendrimer; Phenylactylene; Stilbene; Fluorence; Lifetime

1. Introduction

Intramolecular energy transfer has been an attractive scientific field such as artificial photosynthesis [1]. One of strategies is to link energy donor and acceptor fixed by particular geometry to achieve optimal orientation between transition moments, where the main interaction is confirmed to be through space and through bond involving intervening σ bond [2,3]. The aim of present study is focused on elucidation of energy migration in the dendrimer linked by phenylacetylene units.

Recently, a variety of dendrimers have been synthesized by virtue of new development of synthesis methods [4,5]. Dendrimers bearing multiple chromophores have been developed as a promised candidate due to possibility of efficiently harvesting photons. In this respect, Devadoss et al. have successfully demonstrated efficient energy migration from peripheral moiety to a core chromophore [6]. Furthermore, Aida and co-workers confirmed that efficiency of energy migration between porphyrins in a star-shaped dendrimer is higher than in cone-shaped one, indicating importance of dendrimer shape [7].

We have synthesized enediyne derivatives containing phenylacetylene to investigate cis–trans isomerization and charge transfer reaction in the excited state, and revealed that the dominant feature of these compounds is ascribed to phenylacetylene moieties [8,9]. Present study deals with dendrimers containing stilbene as a core in the result of enediyne works. Target compounds (hereafter abbreviated as *p*-G*n*; $n = 0, 1, 2$) as shown in Fig. 1 were successfully synthesized and identified by ^{1}H NMR and MALDI–TOFMS followed by investigation using steady state absorption and emission spectra as well as fluorescence lifetime measurement.

We found that (1) emissive states of *p*-G1 and *p*-G2 were observed to be almost similar each other, (2) the origin of *p*-G2 emission was attributed to the excited stilbene core generated by energy migration from initially localized peripheral phenylacetylene excited state and (3) rise and decay components were observed and dependent on generation of dendrimer. These results indicate that emissive state of *p*-G*n* is stilbene core and phenylacetylene of *p*-G2 is allowed to interact with stilbene core in the excited state.

2. Experimental

2.1. Apparatus

Sample solutions were prepared in cyclohexane (Kanto Chemical) and benzonitrile (Kanto Chemical) and deoxygenated

---

* Corresponding author. Fax: +81 29 853 4315.
E-mail address: arai@chem.tsukuba.ac.jp (T. Arai).

1010-6030/$ – see front matter © 2005 Published by Elsevier B.V.
doi:10.1016/j.jphotochem.2005.10.041

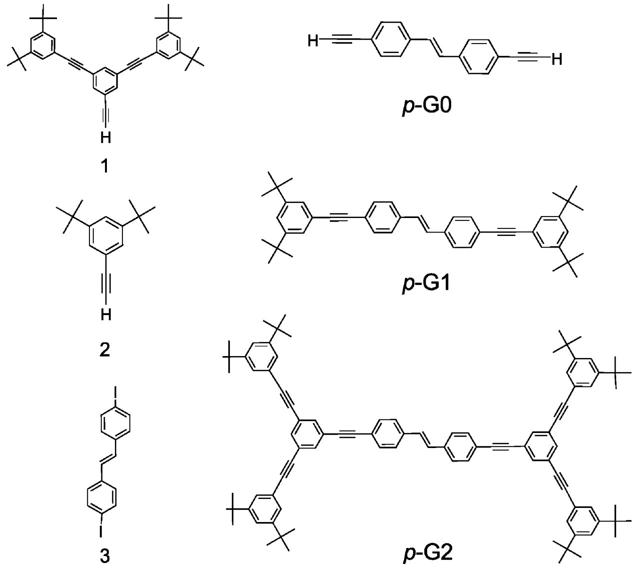

Fig. 1. Reagents and samples.

by bubbling highly purified argon (>99.999%) through a needle. Fluorescence and excitation spectra were measured with Hitachi F-4500 fluorimeter using a 1 cm × 1 cm quartz cuvette. Absorption spectra were recorded with Shimadzu UV-1600 spectrophotometer.

Fluorescence decay measurement was performed by using time-correlated single-photon counting method. The apparatus was assembled based on previous paper [10,11]. Excitation at 410 nm was achieved by a diode laser (PicoQuant, LDH-P-C-405) derived by a power control unit (PicoQuant, PDL 800-B) with a repetition rate of 2.5 MHz. Temporal profiles of fluorescence decay were recorded by using a microchannel plate photomultiplier (Hamamatsu, R3809U) equipped with a TCSPC computer board module (Becker and Hickl, SPC630). Full-width at half-maximum (FWHM) of the instrument response function was 51 ps. Criteria for the best fit were the values of χ^2 and the Durbin–Watson parameters, obtained by nonlinear regression [12].

2.2. Synthesis

p-G0 was synthesized from **3** depicted in Fig. 1 according to the literature [13].

2.2.1. Synthesis of p-G1

A mixture of **3** (0.10 g, 0.23 mmol), dichlorobis (triphenylphosphine) palladium(II) (33 mg, 0.05 mmol), copper(I) iodide (18 mg, 0.09 mmol) and triphenylphosphine (25 mg, 0.09 mmol) in the mixture of toluene (30 ml) and triethylamine (20 ml) was bubbled with nitrogen for 1 h. **2** (130 mg, 0.61 mmol) was added to the solution, and the mixture was stirred under nitrogen at room temperature for 40.5 h [14]. After the reaction was complete, the reaction mixture was poured into water and extracted with dichloromethane. The organic layer was washed with saturated aqueous NH_4Cl, then dried over $MgSO_4$ and filtered. The solvent was evaporated under reduced pressure. And the residue was purified by silica-gel column chromatography (elute: hexane–chloroform = 20:1 to 10:1). The resulting material was purified by recrystallization with ethanol–chloroform to give *p*-G1 62 mg (44%) as a pale yellow crystal. ^1H NMR (400 MHz, $CDCl_3$) δ 1.35 (s, 36H, $-CH_3$) 7.13 (s, 2H, –CH=CH–) 7.39–7.41 (m, 6H, ArH), 7.53 (dd, $J = 8$ Hz, 8H, ArH) ppm. MALDI–TOFMS, found: m/z 604.3 calcd. for $C_{46}H_{52}^+$ 603.4.

2.2.2. Synthesis of p-G2

A mixture of **3** (0.06 g, 0.01 mmol), dichlorobis (triphenylphosphine) palladium(II) (20 mg, 0.03 mmol), copper(I) iodide (11 mg, 0.06 mmol), and triphenylphosphine (15 mg, 0.06 mmol) in the mixture of dichloromethane (20 ml) and triethylamine (10 ml) was bubbled with nitrogen for 1 h. **1** (200 mg, 0.04 mmol) was added to the solution, and the mixture was stirred under nitrogen at room temperature for 53 h [15]. After the reaction was complete, the reaction mixture was poured into water and extracted with dichloromethane. The organic layer was washed with saturated aqueous NH_4Cl, then dried over $MgSO_4$ and filtered. The solvent was evaporated under reduced pressure. And the residue was purified by silica-gel column chromatography (elute: hexane–chloroform = 30:1 to 5:1). The resulting material was purified by recrystallization with hexane–chloroform to give *p*-G2 20 mg (12%) as a pale yellow crystal. ^1H NMR (400 MHz, $CDCl_3$) δ 1.33 (s, 72H, $-CH_3$) 7.13 (s, 2H, –CH=CH–) 7.38 (d, $J = 2$ Hz, 8H, ArH) 7.41 (t, $J = 2$Hz, 4H, ArH) 7.51 (s, 2H, ArH) 7.66 (d, $J = 2$ Hz, 4H, ArH) 7.68 (t, $J = 2$ Hz, 4H, ArH) ppm. MALDI–TOFMS, found: m/z 1228.6 calcd. for $C_{94}H_{100}^+$ 1228.8.

3. Results and discussion

3.1. Steady state spectra

Fig. 2 shows the absorption spectra of *p*-G*n* ($n = 0$, 1, 2) in cyclohexane at room temperature. *p*-G0, which is attributed to a common core part of *p*-G1 and *p*-G2, exhibits slightly progressive structure having a maximum at 336.2 nm accompanied by two distinct shoulders at 323.4 and 353.2 nm. *p*-G1 shows a broader band shape than *p*-G0 and the red-shifted structure maximized at 361.0 nm, arising from difference in electron-donating ability between H and 3,5-di-*tert*-butylphenyl group (BuPh). This is because π-electron of BuPh might be delocalized into a core moiety by resonance interaction. The absorption spectrum of *p*-G2 consists of the superposition of a broad band similar to *p*-G1 and that of phenylacetylene moiety having characteristic progression maximum at 308.6 nm. Another peak of lower energy band is located at 363.6 nm resulting from extended delocalization compared to *p*-G1. There are two shoulders at ∼350 and ∼390 nm in *p*-G1 and *p*-G2, which seem to correspond to shoulders at 323.4 and 353.2 nm in *p*-G0, respectively. The inset of Fig. 2 shows the absorption spectrum of a cis isomer of *p*-G2, of which lower energy band is blue-shifted and has no absorption maximum. Therefore, the broad band maximized at ∼360 nm might generate from prolonged π-conjugation associated with *trans*-stilbene core.

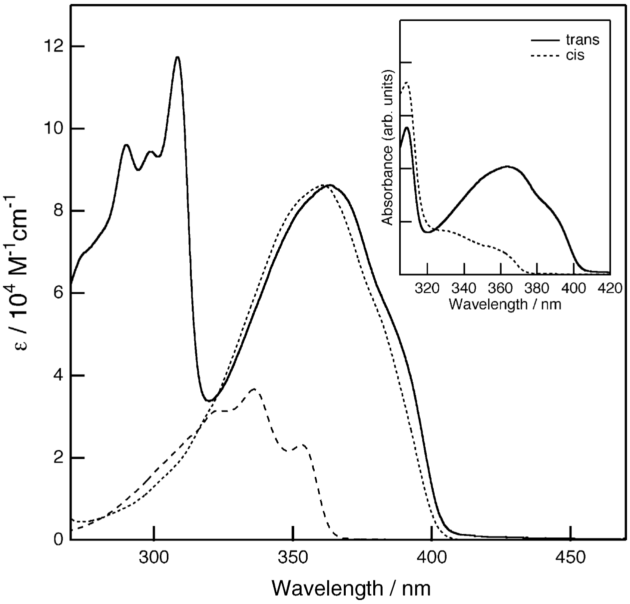

Fig. 2. Absorption spectra of *p*-G0 (broken line), *p*-G1 (dashed line) and *p*-G2 (solid line) in cyclohexane. Inset shows absorption spectra of cis and trans of *p*-G2.

The fluorescence spectra of *p*-G*n* are shown in Fig. 3. The spectral shapes of *p*-G*n* have more distinct progression in fluorescence than in absorption spectra. There are three vibrational peaks at 363.4, 383.0 and 402.6 nm corresponding to 0–0, 0–1 and 0–2 vibrational bands, respectively. A similar vibrational structure was found in *p*-G1 and *p*-G2, of which peaks are located at 401.0 and 424.8 nm, 402.2 and 426.6 nm, respectively, following a shoulder at ~448 nm. The vibrational energy difference between 0–0 and 0–1 was calculated to be ~1400 cm^{-1}, and 0–1 and 0–2 to be ~1200 cm^{-1} for all compounds, leading to be agreement with those of absorption spectra. The small difference in spectral shape between *p*-G1 and *p*-G2 may be ascribed to low electron-donating ability of meta-substituted ethynyl–BuPh in *p*-G2. The fluorescence quantum yields of *p*-G0, G1, G2 in cyclohexane were obtained to be 0.84, 0.82 and 0.83, respectively, using anthracene as a reference compound and found to be almost independent of the dendrimer generation. These values are about 20 times larger than unsubstituted stilbene of 0.04 [16].

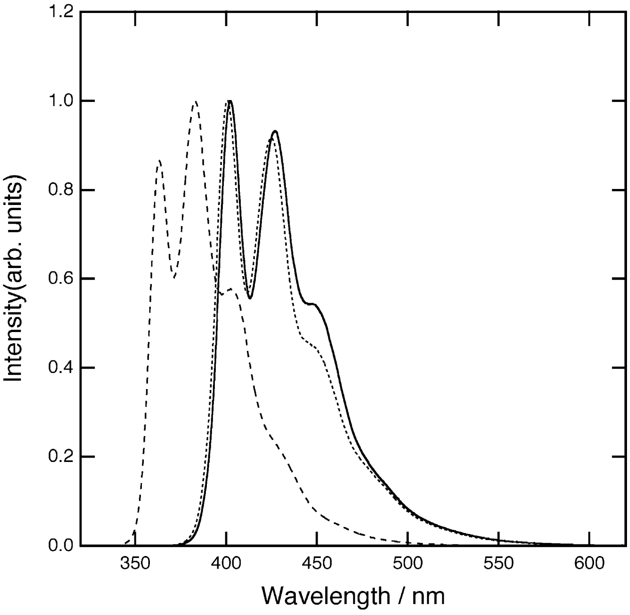

Fig. 3. Fluorescence spectra of *p*-G0 (broken line), *p*-G1 (dashed line) and *p*-G2 (solid line) in cyclohexane. Fluorescence intensity was normalized by maximum intensity.

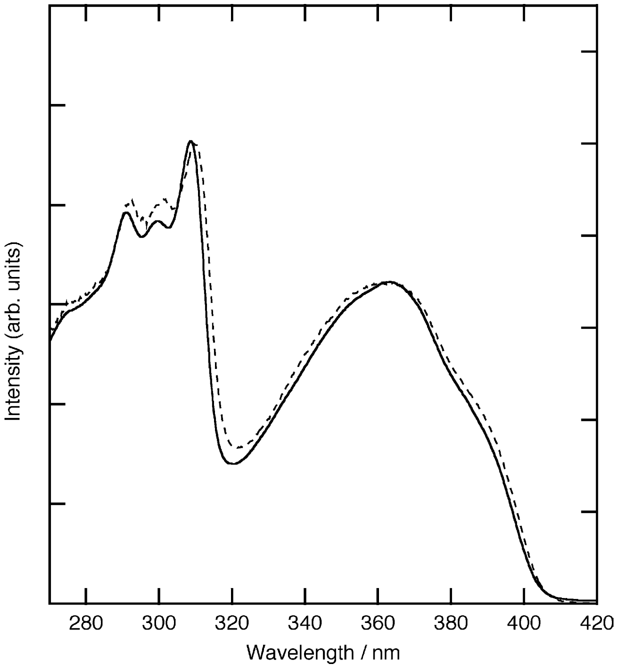

Fig. 4. Fluorescence excitation (broken line) and absorption (solid line) spectra of *p*-G2 in cyclohexane.

Fig. 4 shows fluorescence excitation and absorption spectra of *p*-G2 in cyclohexane. Since *p*-G2 has ethynyl–BuPh units at meta-position in contrast to *p*-G1, absorption spectrum of *p*-G2 consists of two independent chromophores as described above. If there is no interaction in the excited state, excitation spectrum cannot be in agreement with absorption spectrum. Therefore, there may be the considerable interaction between two chromophores in the excited state. In other words, this means that there is no excitation wavelength effect on fluorescence spectra.

3.2. Lifetime analysis

Fluorescence lifetimes of *p*-G1 and *p*-G2 in cyclohexane are listed in Table 1. Both of *p*-G1 and *p*-G2 exhibited biexponential decay consisting of rise and decay components observed both at 425 and 455 nm. Weak wavelength dependence of time constants between 425 and 455 nm was observed for either *p*-G1 or *p*-G2, indicating that the electronic state observed at 425 nm was found to be the same emitting state as at 455 nm. The existence of rise components suggests a certain precursor before forming emissive state. The time constant corresponding to a rise component for *p*-G1 is nearly three times longer than for *p*-G2 in contrast to decay components, reflecting differences in relaxation process

Table 1
Fluorescence lifetime of *p*-G1 and *p*-G2 in cyclohexane and benzonitrile with excitation at 410 nm.

Solvent	Lifetime (ps)			
	425 nm		455 nm	
	Rise	Decay	Rise	Decay
Cyclohexane				
p-G1	96	832	56	811
p-G2	29	654	22	689
Benzonitrile				
p-G1	47	711	52	713
p-G2	39	625	34	629

of *p*-G1 and *p*-G2 in the excited state. The absorbing states of phenylacetylene dendrimers are nearly degenerate as reported by Thompson et al., although a significant splitting of these states takes place in the emitting geometry, which is considered to have a cumulenic structure [17]. If we speculate behaviors of *p*-G1 and *p*-G2 in the excited state, it is necessary to consider a variable coupling between the states as a function of the cumulenic distortion. When *p*-G1 and *p*-G2 relax on the excited state, the differences of couplings between *p*-G1 and *p*-G2 seem to become larger due to the increase of through-bond interaction, reflecting the change in electronic structure. That is, the coupling of *p*-G2 is considered to be larger than that of *p*-G1 due to extended π-conjugation in the excited state, which might affect the differences in rise times of *p*-G1 and *p*-G2.

Lifetimes of *p*-G1 and *p*-G2 in benzonitrile were also measured and showed similar characteristics in cyclohexane; i.e. no monitor wavelength dependence of the time constants was observed for *p*-G1 and *p*-G2. In addition, differences in time constants between *p*-G1 and *p*-G2 are smaller than in cyclohexane. Even though benzonitrile is polar solvent relative to cyclohexane, small solvent dependence of time constants was observed. This indicates that the emissive states of *p*-G1 and *p*-G2 have no remarkable charge transfer character.

3.3. Time-resolved emission spectra

Fig. 5 shows the time-resolved fluorescence spectra of *p*-G1 in cyclohexane with irradiation at 410 nm in the wavelength range 415–550 nm due to excitation wavelength, so that no 0–0 emission band could be measured. Obvious emission maximum and the shoulder were observed at 425 and 445 nm, respectively. Time evolution of fluorescence spectra shows no significant changes in spectral shapes as well as the maximum emission wavelengths. Although a rise component with ∼100 ps was found in *p*-G1 from lifetime analysis, the corresponding spectrum could not be identified. The time-resolved spectra of *p*-G2 are also shown in Fig. 6 in the same measurement condition as *p*-G1. The time evolution of *p*-G2 is similar to *p*-G1 and the relaxation process is considered to be the same as *p*-G1. However, since the rise constant of *p*-G2 is ∼30 ps and faster than that of *p*-G1, ethynyl–BuPh may affect the relaxation time constant of Frank–Condon state of *p*-G2.

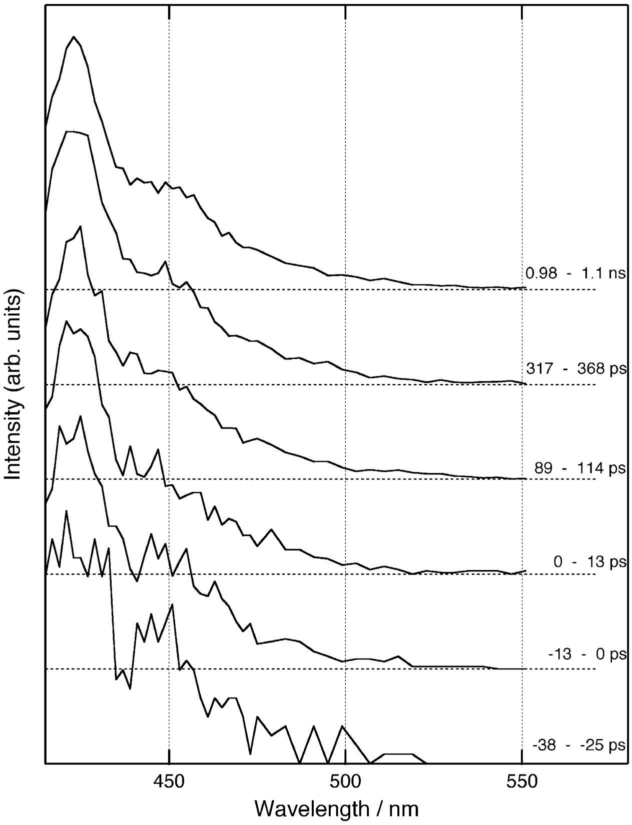

Fig. 5. Time-resolved fluorescence spectra of *p*-G1 in cyclohexane with excitation at 410 nm.

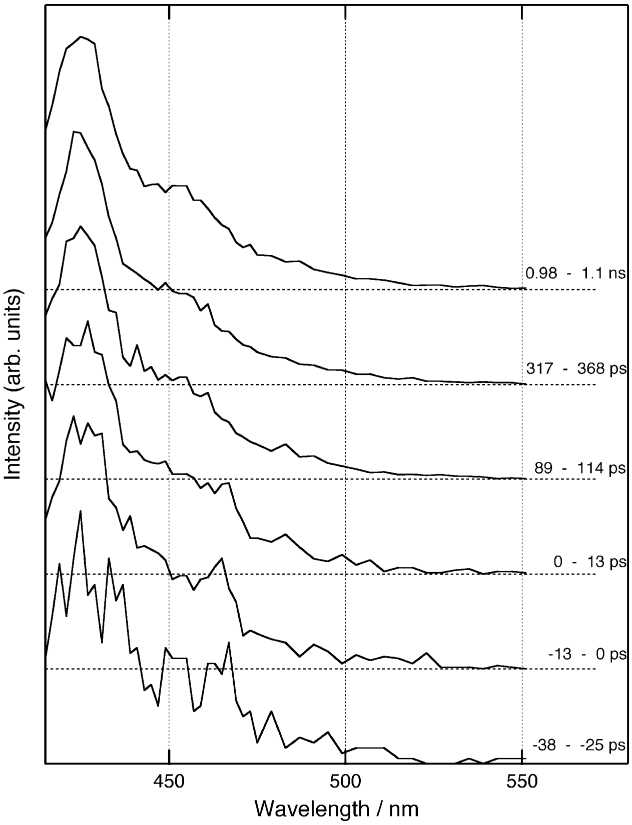

Fig. 6. Time-resolved fluorescence spectra of *p*-G2 in cyclohexane with excitation at 410 nm.

3.4. The origin of emission states of *p*-G*n*

It has been reported that diphenylacetylene (DPA) showed S_1 emission in condensed phase in contrast to S_2 emission in gas phase [18,19]. The absorption spectra of *p*-G*n* shifts to longer wavelength compared to that of DPA and are disagreement with that of DPA exhibiting characteristic progression in absorption spectra. The vibrational structure of *p*-G*n* is similar to that of stilbene rather than that of DPA. In fact, *p*-G0, which is stilbene derivative bearing acetylene at para position of a stilbene unit, seems to show red-shifted spectrum of stilbene by ∼30 nm. The absorption spectrum of *p*-G1 is considered to be broader and more red-shifted spectrum of *p*-G0. Comparison of these fluorescence spectra gives similar spectral shapes to stilbene following red-shift of ∼30 and ∼40 nm relative to stilbene for *p*-G0 and *p*-G1, respectively. Thus, absorption and emission spectra of *p*-G*n* seem to be affected by a stilbene core from consideration of generation dependence of these spectra. *p*-G2, which has ethynyl–BuPh with meta-substitution of *p*-G1, shows the absorption spectrum red-shifted by a few nm to *p*-G1. This means that *p*-G2 has almost the same lowest excited state as *p*-G1; indeed, relaxation process of the excited state of *p*-G2 is considered to show similar manner to that of *p*-G1.

Gaab et al. has reported that the absorption and fluorescence spectra of phenylacetylene derivatives bearing three 3,5-di-*tert*-butylphenyl groups (3-Ph) [20]. 3-Ph has similar electronic state to DPA showing characteristic progression being different from *p*-G*n*. This indicates that stilbene moiety plays an important role in forming the electronic state of *p*-G*n*. The broad absorption and fluorescence spectra may arise from involvement of extended π-conjugation. This also suggests that the origin of emission state is S_1 rather than S_2. Furthermore, 1, 2-bis(phenylethynyl) ethane, which has phenylethynyl moieties instead of phenyl rings of stilbene, exhibits almost the same absorption and fluorescence spectra as DPA being red-shifted by ∼60 nm [8]. In this case, the involved double bond induces the stabilization of the electronic state of phenylacetylene, which dominates absorption and fluorescence spectra like DPA. However, the fluorescence quantum yield of 1,2-bis(phenylethynyl) ethane is larger than DPA and comparable to that of *p*-G*n*. In this sense, the presence of double bond may affect fluorescence quantum yields of compounds containing phenylethynyl moieties.

3.5. The relaxation process of emission states of *p*-G*n*

Rise time constants in every observed wavelength were estimated to be ∼100 and ∼30 ps for *p*-G1 and *p*-G2, respectively, evaluating from lifetime analysis of fluorescence decays and depended on the generation number. In contrast, fluorescence decay constants were analyzed by single exponential function to be ∼800 and ∼700 ps for *p*-G1 and *p*-G2, respectively. This difference might be explained by involvement of meta-substituted ethynyl–BuPh of *p*-G2 in the emissive state, which is considered to be generated from Frank–Condon state by ∼30 ps. It is possible to speculate that the extension of π-conjugation to ethynyl–BuPh moiety in the excited state affects the relaxation constant of *p*-G2 despite of meta-position in *p*-G2. Considering from the difference in rise time constants between *p*-G1 and *p*-G2, there may be some extent of electronic coupling between core and ethynyl–BuPh. From time-resolved fluorescence spectra, the time evolution of spectra shows no time dependence leading to assumption of small change in the electronic structure of the low-lying excited state. Since the rise time constant of *p*-G1 is evidently distinct from that of *p*-G2, one may reasonably speculate that electron-donating ability of ethynyl–BuPh is considered to affect the rise time constant. However, difference in spectral shape of fluorescence between *p*-G1 and *p*-G2 was found to be small, so that it is difficult to distinguish relaxation process of excited states of *p*-G*n* judging from steady state fluorescence spectra.

Thompson et al. have reported that phenylacetylene in the excited state has a cumulenic structure arising from Frank–Condon state. Relatively large Stokes shift of 3-Ph compared to 1-Ph was explained by remarkable structural change in absorption and emission states due to meta-substituted ethynyl–BuPh followed by prolonged π-conjugation including ethynyl–BuPh, i.e. a cumulenic structure [17]. While Stokes shift of *p*-G1 is expected to be small because of similarity of the electronic structure of *p*-G1 to that of 1-Ph, the emission spectrum of *p*-G2 is almost the same as that of *p*-G1 despite of structural similarity of *p*-G2 to 3-Ph. These results suggest that stilbene core is allowed to interact with adjacent phenylacetylene rather than ethynyl–BuPh substituted at meta-position of adjacent one in *p*-G2. Thus, it seems that electronic coupling between stilbene core and ethynyl–BuPh is small even in the excited state. However, excitation spectrum of *p*-G2 consists of sum of the absorption spectra of ethynyl–BuPh and *p*-G1 as shown in Fig. 4, suggesting that there is significant interaction in the emissive state of *p*-G2 such as intramolecular energy migration [1]. On the other hand, singlet energy dissipation can be examined due to red-edge excitation at 410 nm, meaning that there is no excess vibrational energy in lowest excited singlet state of *p*-G2 and excitation is localized around core moiety. The dendrimer-generation dependence of decay constants reveals that ethynyl–BuPh of *p*-G2 also involves in relaxation process in spite of its higher energy level. A cumulenic structure in the excited state is considered to be one of plausible candidates to explain this generation dependence, leading to extension of π-conjugation including stilbene core being no ionic structure. This is consistent with the relatively small difference in relaxation dynamics in between cyclohexane and benzonitrile. Further research will be expected to explore the mechanism of relaxation process of *p*-G*n* by using faster time-resolved spectroscopy besides ethynyl–BuPh excitation.

4. Conclusion

It is concluded that the emissive state of *p*-G*n* is the electronic state associated with core stilbene moiety and highly effective intramolecular energy migration occurs in *p*-G2 from peripheral ethynyl–BuPh to core stilbene followed by emission with high quantum yield. These properties will gives the possibility to prepare light emitting materials bearing light harvesting and emitting parts.

Acknowledgements

This work was supported by a Grant-in-Aid for Scientific Research on Priority Areas (417), the 21st Century COE Program and a Grant-in-Aid for Scientific Research #16550115 from the Ministry of Education, Culture, Sports, Science and Technology (MEXT) of the Japanese Government, by University of Tsukuba Research Projects and by the Asahi Glass Foundation.

References

[1] S. Speiser, Chem. Rev. 96 (1996) 1953–1976.
[2] G.D. Scholes, D.L. Andrews, J. Chem. Phys. 107 (1996) 5374–5384.
[3] G.D. Scholes, K.P. Ghiggino, A.M. Oliver, M.N. Paddon-Row, J. Phys. Chem. 97 (1993) 11871–11876.
[4] C. Gorman, Adv. Mater. 10 (1998) 295–309.
[5] A. Momotake, T. Arai, Polymer 45 (2004) 5369–5390.
[6] C. Devadoss, P. Bharathi, J.S. Moore, J. Am. Chem. Soc. 118 (1996) 9635–9644.
[7] M-S. Choi, T. Aida, T. Yamazaki, I. Yamazaki, Chem. Eur. J. 8 (2002) 2668–2678.
[8] H. Sakakibara, M. Ikegami, K. Isagawa, S. Tojo, T. Majima, T. Arai, Chem. Lett. (2001) 1050–1051.
[9] Y. Miki, A. Momotake, T. Arai, Org. Biomol. Chem. 1 (2003) 2655–2660.
[10] I. Yamazaki, N. Tamai, H. Kume, H. Tsuchiya, K. Oba, Rev. Sci. Instrum. 56 (1985) 1187–1194.
[11] Y. Nishimura, A. Yasuda, S. Speiser, I. Yamazaki, Chem. Phys. Lett. 323 (2000) 117–124.
[12] N. Boens, N. Tamai, I. Yamazaki, T. Yamazaki, Photochem. Photobiol. 52 (1990) 911–917.
[13] N.T. Lucas, E.G.A. Notaras, M.P. Cifuentes, M.G. Humphrey, Organometallics 22 (2003) 284–301.
[14] P. Bharathi, U. Patel, T. Kawaguchi, D.J. Pesak, J.S. Moore, Macromolecules 28 (1995) 5955–5963.
[15] T. Kaneko, T. Horie, M. Asano, T. Aoki, E. Oikawa, Macromolecules 30 (1997) 3118–3121.
[16] J. Saltiel, A.S. Waller, D.F. Sears Jr., J. Am. Chem. Soc. 115 (1993) 2453–2465.
[17] A.L. Thompson, K.M. GaaB, J. Xu, C.J. Bardeen, T.J. Martinez, J. Phys. Chem. A 108 (2004) 671–682.
[18] Y. Hirata, T. Okada, N. Mataga, J. Phys. Chem. 96 (1992) 6559–6563.
[19] K. Okuyama, T. Hasegawa, M. Ito, N. Mikami, J. Phys. Chem. 88 (1984) 1711.
[20] K.M. Gaab, A.L. Thompson, J. Xu, T.J. Martinez, C.J. Bardeen, J. Am. Chem. Soc. 125 (2003) 9288–9289.